

Enhancement of Cavitation Aggressivity around a Cavitating Jet by Injecting Low-Speed Water Jet for Cavitation Peening

Hitoshi SOYAMA
Tohoku University
Sendai, Miyagi, Japan

Kazuto NISHIZAWA
Tohoku University
Sendai, Miyagi, Japan

Mitsuhiro MIKAMI
Tohoku University
Sendai, Miyagi, Japan

ABSTRACT

Cavitation impact at cavitation bubble collapse can be utilized for surface enhancement in the same way as shot peening. A peening method using cavitation impact is called cavitation peening. In the case of cavitation peening, cavitation bubbles were produced by injecting a high-speed water jet into water, i.e., a cavitating jet. In order to improve effect of cavitation peening, enhancement of cavitation aggressivity around a cavitating jet is required. In the present paper, a low-speed water jet was injected around a cavitating jet to increase cavitation aggressivity, as the low-speed water jet eliminate residual bubbles after cavitation bubble collapse. The residual bubble causes cushion effect. The cavitation aggressivity was evaluated by an erosion test using aluminum specimen to assume that large mass loss revealed large aggressivity. The injecting condition of the low-speed water jet was optimized by the erosion test. The arc height which was height of convex curve of Almen strip was also evaluated, as the arc height was normally used to evaluate peening intensity of shot peening. The convex curve was produced by peening as the peened surface was stretched due to plastic deformation. The peening effect was investigated by measurements of residual stress and a plate bending fatigue test using stainless steel specimen. It was revealed that a maximum cumulative erosion rate was increased about 70 % by injecting the low-speed water jet around the cavitating jet at optimum condition. The increasing rate of the arc height induced by the cavitating jet with the low-speed water jet was about five times larger than that of the cavitating jet without the low-speed water jet. The fatigue strength of stainless steel specimen was increased 29 % and 17% peened by the cavitating jet with and without the low-speed water jet comparing to that of non-peened specimen, respectively.

INTRODUCTION

Cavitation impact at cavitation bubble collapse normally

causes severe damage in hydraulic machinery such as pumps, screw propellers and valves. However, the impact can be utilized for the surface modification in the same way of shot peening such as introduction of compressive residual stress and improvement of fatigue strength of metallic materials. A peening method using cavitation impacts is called “cavitation peening” [1] or “cavitation shotless peening” [2 - 8], as shots of shot peening are not required. Cavitation peening successfully introduces compressive residual stress into metallic materials [3, 5, 9 - 12] and it can improve fatigue strength [2, 4, 6 - 8, 13 - 15]. Now it is used to eliminate stress corrosion cracking in nuclear power plants [16]. In the case of cavitation peening, cavitation is produced by injecting a high-speed water jet into water, i.e., a cavitating jet. In view point of practical use of cavitation peening, enhancement of cavitation aggressivity is required to improve peening effect and to shorten processing time.

Although a change of residual stress of impinged by cavitation impact using cavitation tunnel was reported [17], the treatment area was limited. In order to practical use of cavitation impacts, the cavitating jet was proposed [18, 19]. It is possible to produce a cavitating jet in air by injecting a high-speed water jet into a concentric low-speed water jet. Vijey and Brierley made such a jet for cutting rocks [18, 20]. It was reported that Soyama successfully realized a cavitating jet in air for cavitation peening [12]. It was also shown that the cavitating jet in air was more aggressive comparing to normal cavitating jet, i.e., a cavitating jet in water [12, 21, 22]. One of the reasons is that the cavitating jet in air can eliminate residual bubbles after cavitation bubble collapse. When the residual bubbles were recirculated into the cavitating jet, cavitation impact was reduced by the cushion effect. Thus, it might be possible to enhance the cavitation aggressivity by injecting a low-speed water jet without air bubbles around a cavitating jet in water. Although the cavitating jet in air is powerful cavitating jet, it is hard to treat complex shape such as gears. As the water column was broken by the tips

of gear teeth, air was sucked into the cavitating jet and then the cavitating jet did not work. In some cases of practical use of cavitation peening, the cavitating jet in water is useful. Thus, enhancement of cavitation aggressivity of the cavitating jet in water was investigated by injecting a low-speed water jet around the cavitating jet. As the injection of a low-speed water jet around the cavitating jet reduces vorticity around the cavitating jet, the injection condition of the low-speed water jet should be optimized.

When the surface of polycrystalline metallic materials was treated by enhanced cavitation impact, the full width at half maximum of diffracted X-ray profile was decreased [12]. It was confirmed by a fundamental approach of X-ray diffraction method that the micro strain in grains introduced by heat treatment or mechanical finishing was released [23]. The micro strain might be a source of fatigue crack. As mentioned above, the cavitation peening introduces compressive residual stress, which can reduce fatigue crack propagation. It means that enhanced cavitation peening can relieve a source of crack and it reduce crack propagation at the same time. In the view point material science, the enhanced cavitation peening is also interesting phenomenon.

In the present paper, the effect on cavitation aggressivity of injecting a low-speed water jet around the cavitating jet in water was investigated. The cavitation aggressivity was estimated by an erosion test using aluminum specimen. In order to make clear mechanism of enhancement of the cavitation aggressivity, the cavitating jet was observed by a high-speed video camera. The peening effect of the cavitating jet with and without a low-speed water jet was also examined by measurements of residual stress and a plate bending fatigue test using stainless steel specimens.

EXPERIMENTAL SET UP

Figure 1 illustrates schematic diagram of a cavitating jet apparatus for cavitation peening. A low-speed water jet was injected into a water-filled chamber, i.e., tank A, using a turbine pump in tank B. Injection pressure of the low-speed water jet p_L was controlled a rotating speed of an inverter motor of the turbine pump. A high-speed water jet was pressurized by a plunger pump and injected into the low-speed water jet using a concentric nozzle. Injection pressure of the high-speed water jet p_H was controlled by a rotating speed of an inverter motor of the plunger pump. In the present paper, p_H was kept at constant at 30 MPa. As the aggressivity of the cavitating jet was changing with p_L , p_L was chosen as 0.03 MPa considering the result of our previous report [24]. The flow rate for the high-speed and the low-speed water jet was $7.4 \times 10^{-3} \text{ m}^3/\text{min}$ and $4.9 \times 10^{-1} \text{ m}^3/\text{min}$, respectively. The jet power defined by injection pressure and flow rate for the high-speed and the low-speed water jet was 3,700 J and 245 J, respectively.

Figure 2 shows the geometry of nozzles for the high-speed water jet and the low-speed water jet. The diameter d_H for the high-speed water jet was 1 mm. The nozzle for the low-speed water jet was a pipe whose diameter d_L was 50 mm. The clear Lucite pipe was used for an observation of the cavitating jet and stainless steel pipe was used for an erosion test and treatment of stainless steel specimen. The standoff distances s_H and s_L for the high-speed water jet and the low-speed water jet

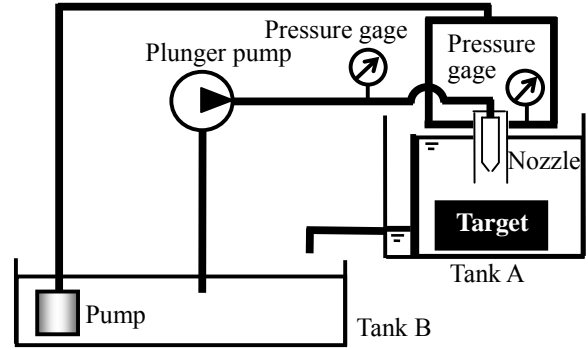


Figure 1: Cavitating jet apparatus for cavitation peening

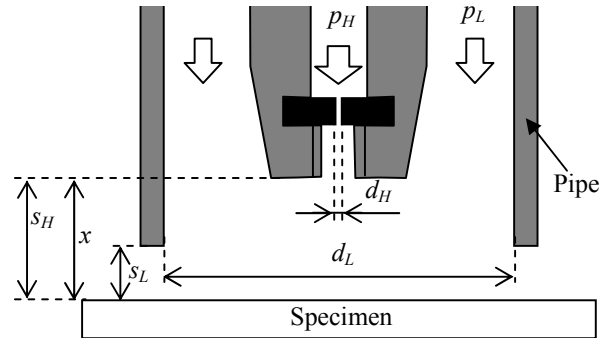


Figure 2: Geometry of nozzle for cavitation jet with low-speed water jet

were defined by the distance from the nozzles to specimen, as shown in Fig. 2. Regarding to our previous paper [24], the ability of the cavitating jet with an associated low-speed water jet was changing with the distance between s_H and s_L , i.e., $s_H - s_L$, s_L , an erosion test was carried out changing with the nozzles distance $s_H - s_L$ and standoff distance s_H .

In order to investigate aggressivity of the cavitating jet, an erosion test was carried out. In the present paper, it was assumed that the large mass loss Δm means the large aggressivity. Material of specimens for the erosion test was pure aluminum (Japan Industrial Standards JIS A1050P). In order to find out the optimum cavitating condition, an exposure time to the cavitating jet was kept constant at 10 minutes, changing with the standoff distance or the nozzle distance.

The aspect of the cavitating jet was observed by using a high-speed video camera, whose maximum sampling rate was 100,000 frames per second. A metal halide lamp was used for the high-speed imaging. In the present experiment, recording conditions were as follows. The sampling rate was 20,000 frames per second and the shutter speed was 5 μs . 1,500 frames, i.e., 74.95 ms, were recorded at each conditions. The images were analyzed using Fourier transformation of intensity at $x = 60 \text{ mm}$ changing with time to investigate shedding frequency of cavitation cloud of the cavitating jet.

When the thin plate was peened, the convex curve was produced as the peened surface was stretched by the plastic deformation. The arc height of the convex curve of Almen strip, which was a thin plate made of spring material, was used as a

parameter of peening intensity for shot peening. In the present experiment, N-gauge of Almen strip was used. The residual stress of stainless steel JIS SUS 316L was also measured by $\sin^2 \psi$ method, which was one of X-ray diffraction methods. The size of specimen was 95 mm X 35 mm with 3 mm in thickness. The cavitating jet scanned with longitudinal direction and the residual stress was measured in longitudinal direction changing with the processing time per unit length t_p . The X-ray tube was operated with a $\text{CrK}\alpha$ X-ray beam at 30 kV and 8 mA. In the present paper, the diffractive plane was the (311) plane of $\gamma\text{-Fe}$, and the diffractive angle without strain, $2\theta_0$, was 148.5 degrees. Diffractive angle measurements from 143 to 153 deg in 0.2 deg steps were made. The iso-inclination method was used for the measurement, and X-rays were counted for 4 s for each step using a scintillation counter. The angles between the normal to the surface and the normal to the lattice plane, ψ , were 0, 22.8, 33.2, 42.1 and 50.7 deg, respectively, and the value of ψ was constant between the measurements at each angle ψ . Under the present conditions, the stress factor was $-369.5 \text{ MPa/degrees}$.

RESULTS

Figure 3 illustrates the mass loss Δm as a function of standoff distance s_H for the cavitating jet with the low-speed water jet, the cavitating jet with pipe of the low-speed water jet without injection of the jet and the cavitating jet without pipe without the injection of the jet. In the case of the cavitating jet with the low-speed water jet, the three cases changing with the nozzle distance, i.e., $s_H - s_L = 20, 30$ and 40 mm were shown in Fig. 3. The nozzle distance for the the cavitating jet with pipe was set at 30 mm , as the mass loss of the cavitating jet with the low-speed water jet at $s_H - s_L = 30$ shows the maximum in Fig. 3. For all cavitating jet with the low-speed water jet and the cavitating jet with and without pipe, the mass loss was increased with the standoff distance s_H , and it had a maximum at $s_H = 60$ or 65 mm , and then decreased. The standoff distance where the mass loss had a maximum was called an optimum standoff distance. The mass loss of the cavitating jet with the low-speed water jet was larger than those of the cavitating jet with and without pipe. The mass loss of the cavitating jet with the low-speed water jet at $s_H - s_L = 30$ was larger than the other cases, i.e., $s_H - s_L = 20$ and 40 mm . The cavitating jet of $s_H - s_L = 30$ at the optimum standoff distance was about 10 times larger than that of the cavitating jet without pipe. It was also 4 times larger than that of the cavitating jet with pipe without injection. The injection of the low-speed water jet around the cavitating jet increases aggressivity of the cavitating jet. It was also note that the mass loss was increased by about two times by setting the pipe.

In order to compare the aggressivity of the cavitating jet, the cumulative erosion rate should be considered, as the cavitation erosion stages was divided into four stages, i.e., incubation stage, acceleration stage, steady state stage and attenuation stage. Figure 4 shows the mass loss changing with the exposure time to the cavitating jet for the cavitating jet without pipe and the cavitating jet with the low-speed water jet. The standoff distance s_H was 60 mm of the cavitating jet without pipe. The conditions of the cavitating jet with the low-speed water jet were follows; s_H was 60 mm and $s_H - s_L$ was 30 mm . Both cavitating jets show

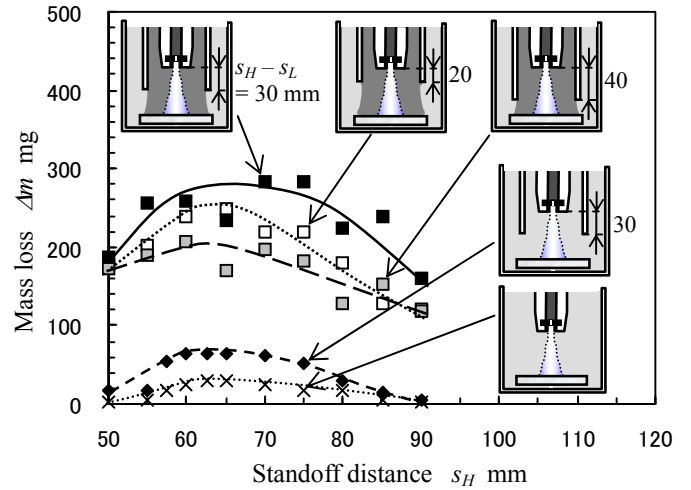


Figure 3: Mass loss changing with standoff distance for cavitating jet with and without low-speed water jet

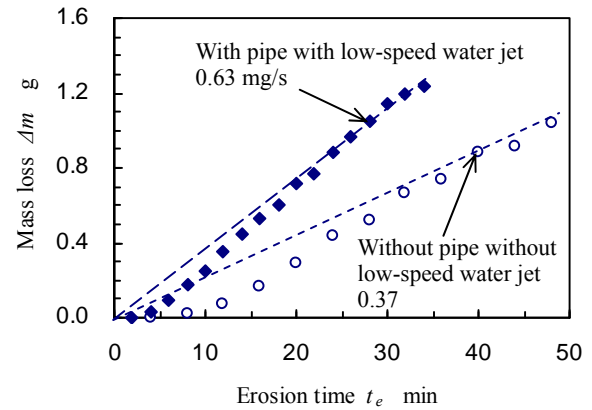
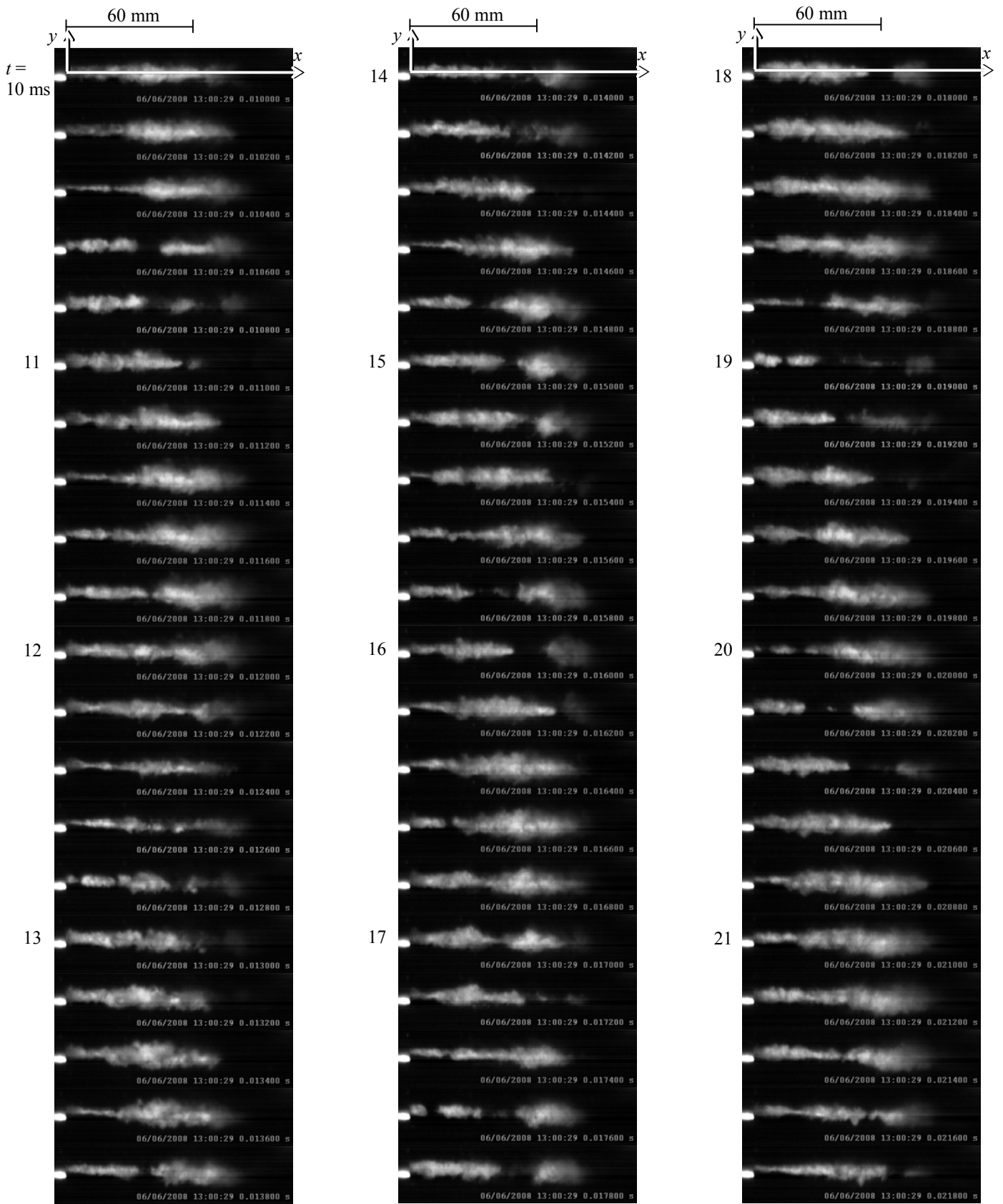


Figure 4: Mass loss changing with erosion time for cavitating jet with and without low-speed water jet

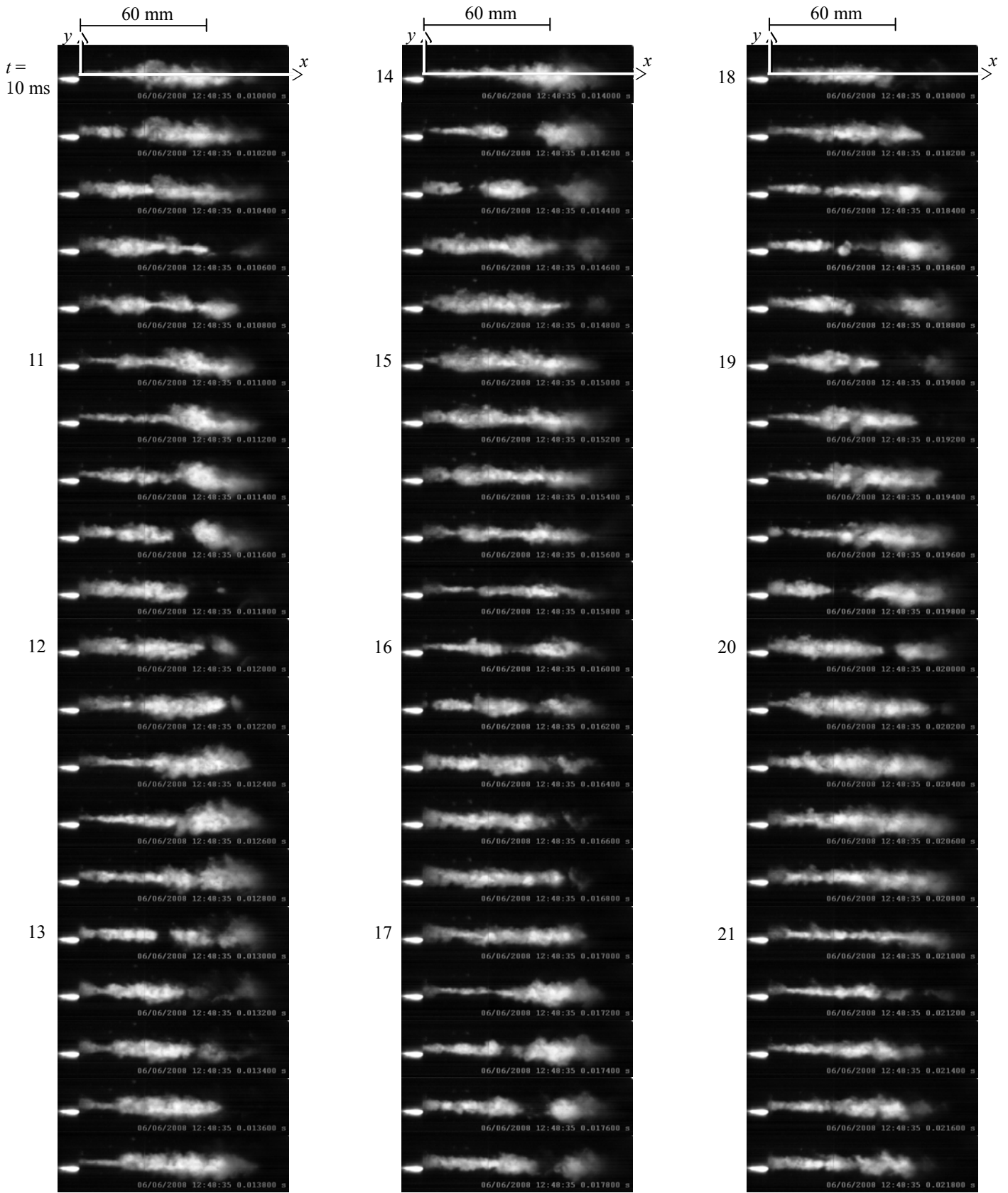
incubation stage, acceleration stage, steady state stage and attenuation stage changing with the erosion time. The maximum cumulative erosion rate of the cavitating jet without pipe was 0.37 mg/s and that of the cavitating jet with the low-speed water jet was 0.63 mg/s . This means that the aggressivity of the cavitating jet with the low-speed water jet was about 70 % larger than that of the cavitating jet without pipe. In Fig. 3, the difference of the aggressivity of the cavitating jet with and without the low-speed water jet was about ten times, as the erosion time was 10 minutes and the erosion stage of the cavitating jet without pipe was incubation stage. In any case, the low-speed water jet around the cavitating jet enhanced the aggressivity of the cavitating jet. The low-speed water jet around the cavitating jet eliminates recirculating bubbles after cavitation bubble collapses and it reduces cushion effect. As the pressure on the surface of the erosion specimen was increased by impinging of the low-speed water jet, the cavitation cloud collapses severely because of high-surrounding pressure. These are the reasons why the injection of the low-speed water jet increases aggressivity of the cavitating jet.

Figure 5 reveals the aspect of the cavitating jet without



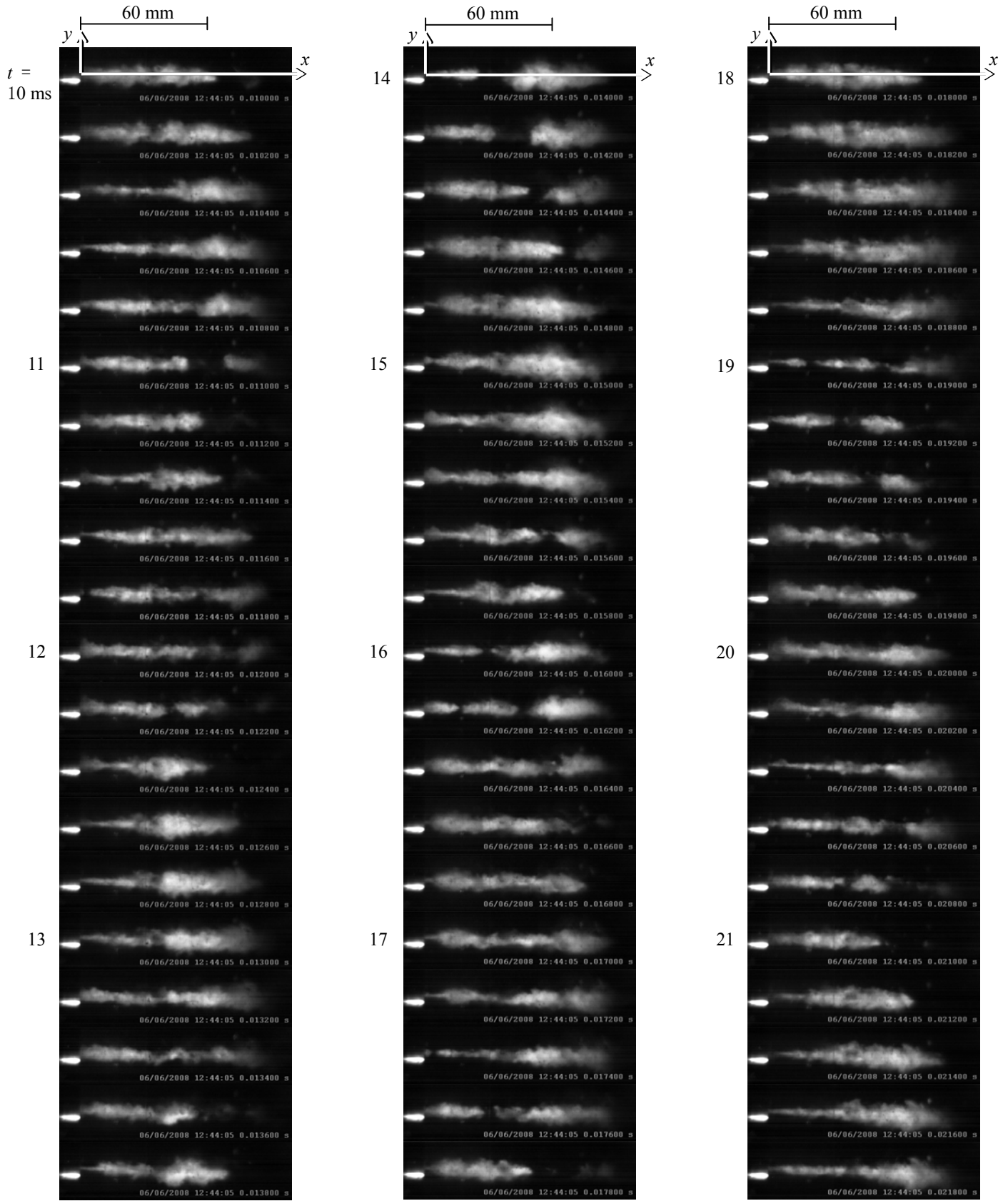
(a) Without pipe without low-speed water jet

Figure 5: Aspect of cavitating jet changing with time



(b) With pipe without low-speed water jet

Figure 5: Aspect of cavitating jet changing with time (continued)



(c) With pipe with low-speed water jet

Figure 5: Aspect of cavitating jet changing with time (continued)

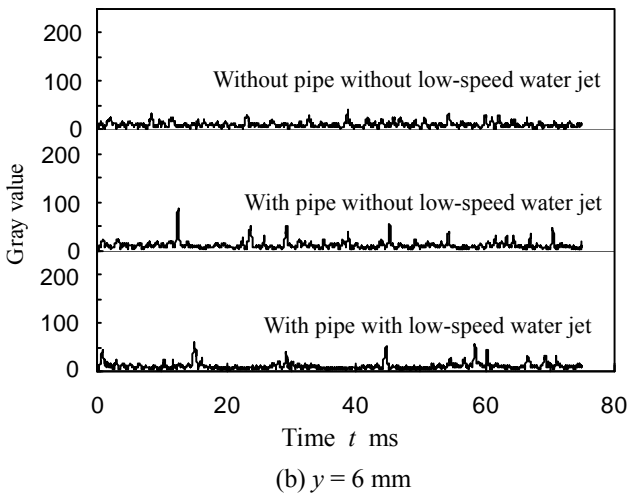
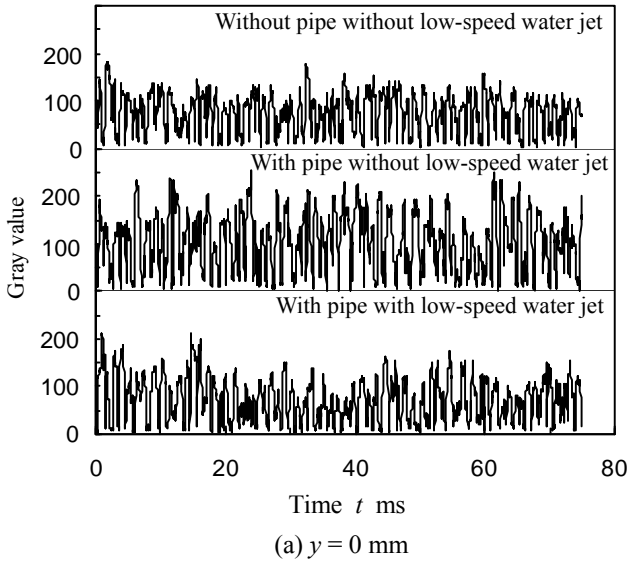


Figure 6: Gray scale of images changing with time corresponding to cloud shedding ($x = 60$ mm)

pipe, the cavitating jet with pipe without injection and the cavitating jet with the low-speed water jet, in order to investigate why the low-speed water jet enhanced the aggressivity of the cavitating jet. The nozzle for injecting the high-speed water jet was shown left hand side in Fig. 5. The direction of flow was left to right. The clear Lucite pipe was used for injecting the low-speed water jet. The white region reveals the cavitation cloud consist of small bubbles. The cavitation clouds were shedding periodically as shown in the previous report [25]. As shown in Fig. 5 (a), the cavitating region was developed and then broken around $x = 40$ mm, at $t = 10.6, 11.8, 12.8, 13.8, 14.8, 15.8, 17, 17.8, 19, 20.2$ and 21.4 . The breaks were occurred at about 1 ms interval, i.e., 1 kHz. In the case of the cavitating jet with pipe, the breaks were occurred around $x = 50$ mm, at $t = 11.6, 13.0, 14.2, 16.0, 17.6, 18.8$ and 19.8 . Although the frequency of the breaks was about 1 kHz, the sub-harmonic frequency was also observed. The width of the cloud cavitation became large at $t = 11.2 - 11.6$

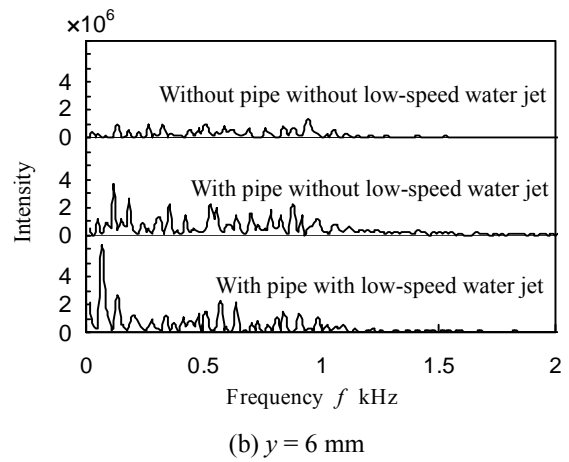
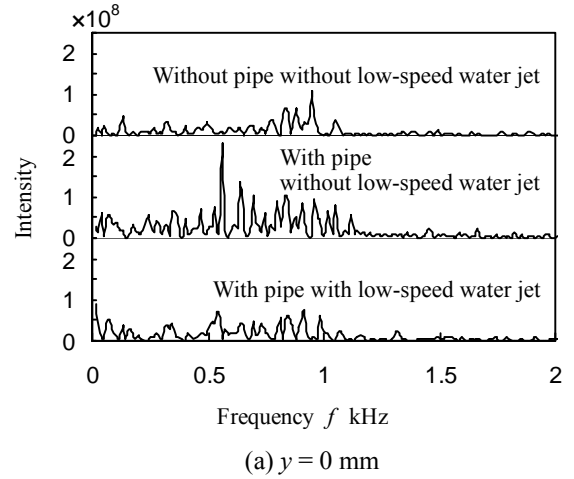


Figure 7: Shedding frequency obtained by image analysis ($x = 60$ mm)

ms. In the case of the cavitating jet with the low-speed water jet, the cavitating region was broken around $x = 60$ at $t = 11, 12.4, 13.6, 14.4, 15.6, 16.2, 17.8, 19.0$ and 20.6 . Although the frequency of the breaks was similar as the cavitating jet with and without pipe, the huge cavitation cloud was observed at $t \approx 15$ ms. The basic frequency of the breaks, i.e., the shedding frequency of the cavitation cloud was similar for all three cases. In the case of the cavitating jet with pipe even though without injection, the huge cavitation cloud was generated some times. The huge cavitation cloud might produce the huge impact at bubble collapse.

In order to investigate the shedding frequency of the cavitation cloud, the gray values of each image as a function of time was shown in Fig. 6 and the results of Fourier transformation of them were illustrated in Fig. 7 for all three cavitating jet. The gray values of position at $(x, y) = (60 \text{ mm}, 0 \text{ mm})$ and $(60 \text{ mm}, 6 \text{ mm})$ were picked up and analyzed, as the optimum standoff distance was about 60 mm. The reason why the gray scale of the images at $y = 6$ mm was chosen is that the gray scale of the images at $y = 6$ mm would be changed, when the huge cavitation cloud was developed. The basic frequency of cavitation cloud shedding was about 1 kHz, as shown in Fig. 7 (a). When the huge cavitation cloud was developed, the gray

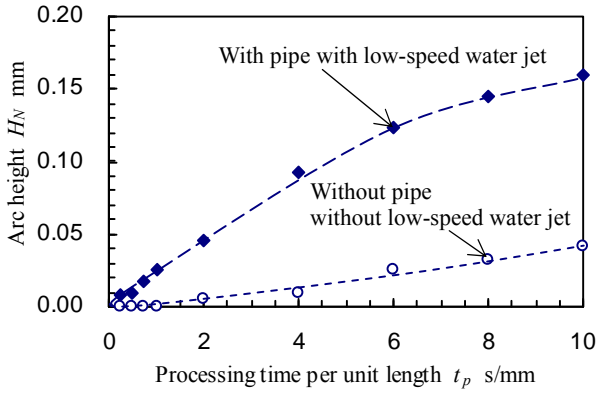


Figure 8: Arc height induced by cavitating jet

value in Fig. 6 (b) was increased. For example, the gray scale of the cavitating jet with pipe at $t \approx 11$ ms and the cavitating jet with the low-speed water jet at $t \approx 15$ ms was increased. The generation interval of the huge cavitation cloud was 10 ms and their frequency was about 100 Hz. As shown in Fig. 7 (b), the intensity at several hundreds Hz was increased at $(x, y) = (60$ mm, 6 mm) for the cavitating jet with pipe and the cavitating jet with the low-speed water jet. This means that these two cavitating jet can produce the huge cavitation cloud and it might cause huge impact. This would be one of the reasons why the aggressivity of the cavitating jet with the pipe and the cavitating jet with the low-speed water jet was larger than that of the cavitating jet without pipe. Considering the effect of residual stress mentioned above, the aggressivity of the cavitating jet with pipe without injection was enhanced by the size of the cavitation cloud. On the other hand, in the case of a cavitating jet with the low-speed water jet, the size of cavitation cloud and elimination of residual bubble are increased the cavitation aggressivity.

In order to investigate peening effect of injection of the low-speed water jet around the cavitating jet, the arc height of Almen strip was shown in Fig. 8. In the case of the arc height, the larger arc height means better peening effect. Both cavitating jets with and without the low-speed water jet reveal peening effect, as the arc height increased with the processing time per unit length. In the case of the cavitating jet with the low-speed water jet, the arc height increased with the processing time linearly at $t_p < 4$ s/mm and then it would be saturated. On the other hand, in the case of the cavitating jet without pipe, the arc height increases the processing time at $t_p \leq 10$ s/mm. The increasing rate of the arc height within the linearly region of the cavitating jet with the low-speed water jet was $23 \mu\text{m/s}$ and that of the cavitating jet without pipe was $4.2 \mu\text{m/s}$. Namely, in the view point of peening intensity using increasing rate of the arc height, the peening intensity of the cavitating jet with the low-speed water jet was 5 times larger than that of the cavitating jet without pipe. In view point of saturated arc height, the peening intensity of the cavitating jet with the low-speed water jet would be about two times larger than that of the cavitating jet without pipe.

Figure 9 illustrates the residual stress changing with the processing time per unit length, as the cavitating jet was using in the nuclear power plants to eliminate stress corrosion

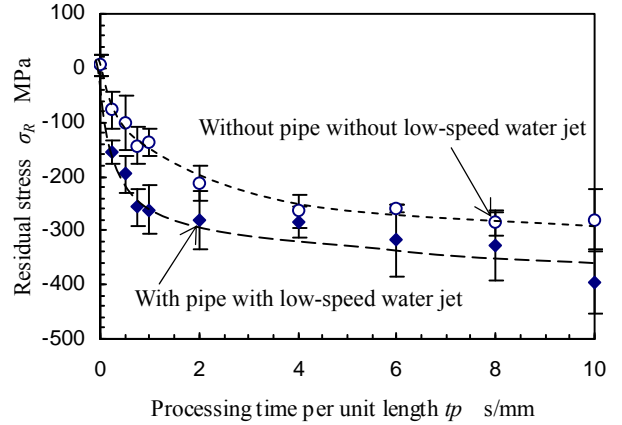


Figure 9: Introduction of compressive residual stress induced by cavitating jet

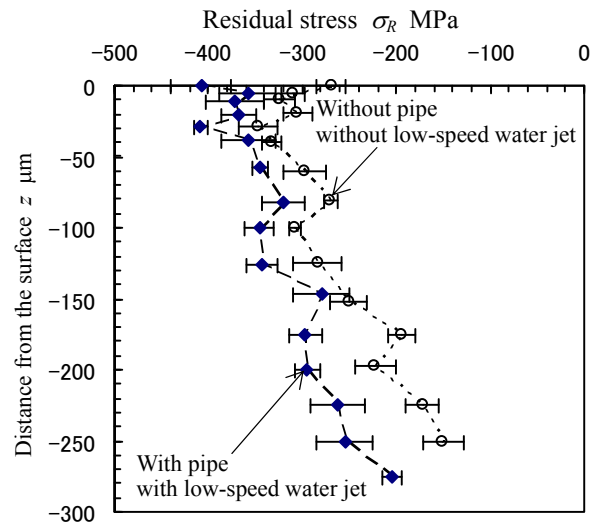


Figure 10: Distribution of residual stress changing with depth

cracking SCC by introducing compressive residual stress [16]. Both cavitating jets introduced compressive residual stress on the surface of the stainless steel. The compressive residual stress was increased and then saturated in the both cases. The saturated compressive residual stress of the cavitating jet with the low-speed water jet was 400 MPa and that of the cavitating jet without pipe was 300 MPa. In the short processing time, the cavitating jet with the low-speed water jet introduces -200 MPa within $t_p < 0.5$ s/mm. It takes about $t_p = 2$ s/mm for the cavitating jet without pipe. These mean that the cavitating jet with the low-speed water jet was more effective to introduce compressive residual stress.

Figure 10 illustrates the distribution of the residual stress in the stainless steel at $t_p = 10$ s/mm for both cavitating jets. Although both cavitating jets introduce compressive residual stress, the compressive residual stress introduced by the cavitating jet with the low-speed water jet was about more 100MPa larger at same depth than that of the cavitating jet without pipe. The cavitating jet with the low-speed water jet can introduce compressive residual stress deeper than the

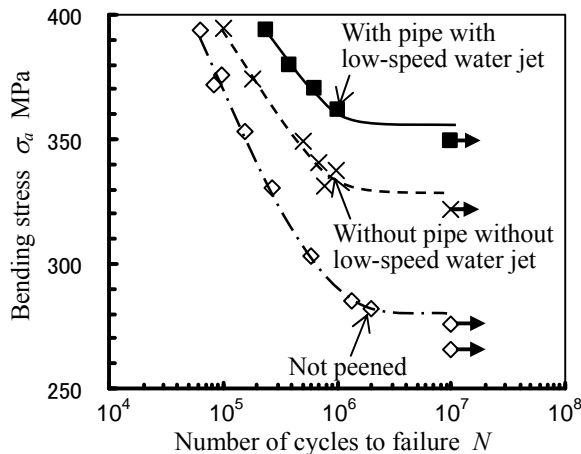


Figure 11: Improvement of fatigue strength of stainless steel by the cavitating jet

cavitating jet without pipe.

Figure 11 reveals the results of a plate bending fatigue test using stainless steel specimen. In the case of peened specimen, the processing time per unit length was 10 s/mm. The number of the cycles to failure at high amplitude was improved by peening using both cavitating jet. The fatigue strength was also improved by the cavitating jet. When the fatigue strength at 10^7 was obtained by using Little's method [26], the fatigue strength of not peened specimen was 279 MPa, that of the specimen peened by the cavitating jet with the low-speed water jet was 360 MPa, and that of the specimen peened by the cavitating jet without pipe was 327 MPa. The cavitating jet without pipe improved fatigue strength of stainless steel about 17 % and the cavitating jet with the low-speed water jet improved about 29 %. Although both peening by both cavitating jets improved the fatigue strength, the cavitating jet with the low-speed water jet was more effective. Namely, the fatigue strength peened by aggressive cavitating jet reveals better fatigue strength.

CONCLUSIONS

In order to enhance the aggressivity of the cavitating jet, the low-speed water jet was injected around the cavitating jet to increase peening effect. The aggressivity was evaluated by the erosion test using aluminum specimen. The mechanism of enhancement of the aggressivity of the cavitating jet was investigated by the observation of the cavitating jet using the high-speed video camera and image analysis. The peening effects were confirmed by measurements of the arc height of Almen strip and the residuals stress of the stainless steel. The fatigue strength of the stainless steel was also evaluated. The main results are summarized as follows:

(1) The injecting of the low-speed water jet around the cavitating jet enhances the aggressivity of the cavitating jet at the following condition; the injection pressure of the high-speed water jet was 30 MPa, the nozzle for the high-speed water jet was 1 mm in diameter; the injection pressure of the low-speed water jet was 0.03 MPa and the nozzle for the low-speed water jet was 50 mm in diameter, the distance between the nozzles was 30 mm.

- (2) The cumulative erosion rate using aluminum specimen of the cavitating jet with the low-speed water jet at optimum condition was 70% larger than that of the cavitating jet without pipe for the low-speed water jet. The low-speed water jet might reduce cushion effect induced by the residual bubbles after cavitation bubble collapses.
- (3) In the case of the cavitating jet with the low-speed water jet at optimum condition and the cavitating jet with pipe without injection, the huge cavitation clouds was developed at several hundreds Hz in frequency. The huge cavitation cloud might produce large impact at bubble collapse.
- (4) The aggressive cavitating jet with the low-speed water jet at optimum condition produces large arc height of Almen strip and introduces more compression into stainless steel.
- (5) The cavitating jet without pipe for the low-speed water jet improved fatigue strength of stainless steel specimen about 17 % comparing to the non-peened specimen. The cavitating jet with the low-speed water jet at optimum condition improved 29 %. Namely, the aggressive cavitating jet produces better peening effect.

ACKNOWLEDGEMENTS

This work was partly supported by the Japan Society for the Promotion of Science under a Grant-in-Aid for Scientific Research (A) 20246030 and The MIKIYA Science and Technology Foundation.

REFERENCES

- [1] Soyama, H. 2006, "Surface Modification of Metallic Materials by Cavitation Peening," *Materia Japan*, 45, 657-663 (in Japanese).
- [2] Soyama, H., Saito, K. and Saka, M. 2002, "Improvement of Fatigue Strength of Aluminum Alloy by Cavitation Shotless Peening," *Journal of Engineering Materials and Technology, Trans. ASME*, 124, 135-139.
- [3] Soyama, H., Sasaki, K., Odhiambo, D. and Saka, M. 2003, "Cavitation Shotless Peening for Surface Modification of Alloy Tool Steel," *JSME International Journal, Series A*, 46, 398-402.
- [4] Odhiambo, D. and Soyama, H. 2003, "Cavitation Shotless Peening for Improvement of Fatigue Strength of Carbonized Steel," *International Journal of Fatigue*, 25, 1217-1222.
- [5] Soyama, H., Macodiyo, D. O. and Mall, S. 2004, "Compressive Residual Stress into Titanium Alloy Using Cavitation Shotless Peening Method," *Tribology Letters*, 17, 501-504.
- [6] Soyama, H. and Macodiyo, D.O. 2005, "Fatigue Strength Improvement of Gears Using Cavitation Shotless Peening," *Tribology Letters*, 18, 181-184.
- [7] Soyama, H., Shimizu, M., Hattori, Y. and Nagasawa, Y. 2008, "Improving the Fatigue Strength of the Elements of a Steel Belt for CVT by Cavitation Shotless Peening," *Journal of Materials Science*, 43, 5028-5030.
- [8] Seki, M., Soyama, H., Fujii, M. and Yoshida, A. 2008, "Rolling Contact Fatigue Life of Cavitation-Peened Steel Gear," *Tribology Online*, 3, 116-121.
- [9] Soyama, H. Yamauchi, Y., Ikohagi, T., Oba, R., Sato, K., Shindo, T. and Oshima, R. 1996, "Marked

- Peening Effects by Highspeed Submerged-Water-Jets,” *Journal of Jet Flow Engineering* (in Japanese), 13-1, 25-32.
- [10] Hirano, K., Enomoto, K., Hayashi, E. and Kurosawa, K. 1996, “Effects of Water Jet Peening on Corrosion Resistance and Fatigue Strength of Type 304 Stainless Steel,” *Journal of the Society of Materials Science, Japan* (in Japanese), 45, No. 7, 740-745.
- [11] Soyama, H., Park, J. D. and Saka, M. 2000, “Use of Cavitating Jet for Introducing Compressive Residual Stress,” *Journal of Manufacturing Science and Engineering, Trans. ASME*, 122, 83-89.
- [12] Soyama, H. 2004, “Introduction of Compressive Residual Stress Using a Cavitating Jet in Air,” *Journal of Engineering Materials and Technology, Trans. ASME*, 126, 123-128.
- [13] Soyama, H. 2000, “Improvement in Fatigue Strength of Silicon Manganese Steel SUP7 by Using a Cavitating Jet,” *JSME International Journal*, 43, Series A, No. 2, 173-178.
- [14] Soyama, H., Kusaka, T. and Saka, M. 2001, “Peening by the use of cavitation impacts for the improvement of fatigue strength,” *Journal of Materials Science Letters*, 20, No. 13, 1263-1265.
- [15] Soyama, H., Sekine, Y. and Oyama, Y. 2008, “Improvement of the Fatigue Strength of Stainless Steel SUS316L by a Cavitating Jet with an Associated Water Jet in Water,” *ISIJ International*, 48, No.11, 1577-1581.
- [16] Saitou, N., Enomoto, K., Kurosawa, K., Morinaka, R., Ishikawa, T. and Yoshimura, T. 2003, “Development of Water Jet Peening Technique for Reactor Internal Components of Nuclear Power Plant,” *Journal of Jet Flow Engineering* (in Japanese), 20, No. 1, 4-12.
- [17] Blickwedel, H., Haferkamp, H., Louis, H. and Tai, P. T. 1987, “Modification of Material Structure by Cavitation and Liquid Impact and Their Influence on Mechanical Properties,” *Proceedings of 7th International Conference on Erosion by Liquid and Solid Impact, Cambridge*, 31-1-31-6.
- [18] Vijey, M. M. and Brierley, W. H. 1978, “Cutting Rocks and Other Materials by Cavitating and Non-Cavitating Jets,” *Proceedings of 4th International Symposium on Jet Cutting Technology*, No. C5, 51-66.
- [19] Yamauchi, Y., Soyama, H., Adachi, Y., Sato, K., Shindo, T., Oba, R., Oshima, R. and Yamabe, M. 1995, “Suitable Region of High-Speed Submerged Water Jets for Cutting and Peening,” *JSME International Journal*, 38, Series B, 245-251.
- [20] Vijey, M. M., Bai, C., Yan, W. and Tieu, A. 2001, “Reverse Flow Nozzle for Generating Natural Cavitating or Pulsed Waterjets: Basic Study and Applications,” *Proceedings of 15th International Conference on Jetting Technology*, 1-17.
- [21] Soyama, H. 2005, “High-Speed Observation of a Cavitating Jet in Air,” *Trans. ASME, Journal of Fluids Engineering*, 127, 1095-1101.
- [22] Soyama, H. 2007, “Improvement of fatigue strength by using cavitating jets in air and water,” *Journal of Materials Science*, 42, No. 16, 6638-6641.
- [23] Soyama, H. and Yamada, N. 2008, “Relieving Micro-Strain by Introducing Macro-Strain in a Polycrystalline Metal Surface by Cavitation Shotless Peening,” *Materials Letters*, 62, No. 14, 3564-3566.
- [24] Soyama, H. and Mikami, M. 2007, “Improvement of Fatigue Strength of Stainless Steel by Using a Cavitating Jet with an Associated Water Jet in Water,” *Key Engineering Materials*, 353-358, 162-165.
- [25] Soyama, H., Yamauchi, Y., Adachi, Y., Sato, K., Shindo, T. and Oba, R., 1995, “High-Speed Observations of the Cavitation Cloud around a High-Speed Submerged Water Jet,” *JSME International Journal*, 38B, 245 - 251.
- [26] Little, R.E. 1972, “Estimating the Median Fatigue Limit for Very Small Up-and-Down Quantal Response Tests and for *S-N* Data with Runouts,” *ASTM STP 511*, 29-42.